An Investigation of a Balanced Hybrid Active-Passive Actuator for Physical Human-Robot Interaction

Patrick Dills[1], Alexander Dawson-Elli[1], Kreg Gruben[2], Peter Adamczyk[1], *Member, IEEE*, Michael Zinn[1], *Member, IEEE*

***Abstract*— Cooperative robots or "cobots" promise to allow humans and robots to work together more closely while maintaining safety. However, to date the capabilities of cobots are greatly diminished compared to industrial robots in terms of the force and power they are able to safely produce. This is in part due to the actuation choices of cobots. Low impedance robotic actuators aim to solve this problem by attempting to provide an actuator with a combination of low output impedance and a large bandwidth of force control. In short the ideal actuator has a large dynamic range. Existing actuators success and performance has been limited. We propose a high force and high power balanced hybrid active-passive actuator which aims to increase the actuation capability of low impedance actuators and to safely enable high performance larger force and workspace robots. Our balanced hybrid actuator does so, by combining and controlling a series elastic actuator, a small DC motor, and a particle brake in parallel. The actuator provides low and high frequency power producing active torques, along with power absorbing passive torques. Control challenges and advantages of hybrid actuators are discussed and overcome through the use of trajectory optimization, and the safety of the new actuator is evaluated.**

***Index Terms*— Human-Robot Interaction, Actuation**

I. Introduction

In recent years robotic manipulators have been delegated tasks which bring them into increasingly closer contact with people. Prime examples include the proliferation of manufacturing cobots, human exoskeletons, and rehabilitation robots [1]. Existing systems are not well suited to applications that require high force (>30-150N) and high power (>60-600 watts) while also maintaining the physical characteristics important for safe and effective physical interaction and human-robot collaboration.

While much progress has been made in co-robotics, the overwhelming focus has been on robotic manipulators which have relatively low power capacity, such that the inherent safety risks when working directly with humans are minimized. The focus has been on the design and control of naturally light weight and compliant manipulators [2]. In this case, human-robot physical interaction and cooperation is enabled via the manipulator's naturally low output impedance, which both facilitates the control of robot-human physical interaction and limits the total energy transferred during an uncontrolled collision between a robot and a human (the greatest safety risk) [3].

Unfortunately, the control and design approach applied to low power systems does not scale to manipulators with high force, power, and bandwidth requirements. Due primarily to the limitations of actuation technology [4], high power manipulators must employ transmission designs to achieve the forces and stiffness required. Such designs are can cause an unsafe amount of output impedance.

To enable high-performance robot-human interaction, the output impedance of high-power manipulators must be reduced to levels sufficient to guarantee inherent safety and to enable human-robot physical interaction without sacrificing the characteristics important to manipulation tasks. Researchers have investigated the use of active force and impedance control [5], which has been used widely in low-power manipulators. However, in high-power systems, force or impedance control is limited by the manipulator's lack of self-sensing capability (motor torque measurements cannot be used reliably to estimate contact forces), a capability inherent to low-power co-robotic manipulators. Even when feedback control is used, such as instrumenting the manipulator's end-effector with a force/torque sensor used in feedback [6], the improved performance is limited to point-to-point interactions at the end effector and is only effective below the feedback control bandwidth.

To simultaneously realize high power and low output impedance, researchers have explored the use of a diverse range of variable impedance actuation strategies [5]. Active compliant actuation, such as the series elastic actuator (SEA) [4][7][8], variable stiffness actuators [9], and variations on these designs place an elastic element in between a speed reducer and the actuator output. Output impedance is reduced through control resulting in a power dense torque source

Manuscript received: October 15, 2020; Revised January 16, 2021; Accepted February 16,2021

This paper was recommended for publication by Editor Gentiane Venture upon evaluation of the Associate Editor and Reviewers' comments. This work was supported by the National Science Foundation (grant: NSF 1830516)

[1] Patrick Dills,Alexander Dawson-Elli, Peter Adamczyk, and Michael Zinn are with the Mechanical Engineering Department, University of Wisconsin – Madison . pdills| dawsonelli| mzinn| peter.adamczyk|@wisc.edu

[2] Kreg Gruben is with the the Deparment of Kinsesiology, University of Wisconsin – Madison. kreg.gruben@wisc.edu

© 2021 IEEE. Personal use of this material is permitted. Permission from IEEE must be obtained for all other uses, in any current or future media, including reprinting/republishing this material for advertising or promotional purposes, creating new collective works, for resale or redistribution to servers or lists, or reuse of any copyrighted component of this work in other works

below the control bandwidth of the actuator. Attempts to extend the performance of series elastic actuators have been made with some success by including a small secondary motor on the output to extend the torque frequency range of the actuator as a whole [3].

More recently hybrid actuation, the combination of controlled passive actuators, such as brakes or dampers, and active actuators, such as electric motors, has demonstrated advantages including high passive force capability, energy efficiency, low output impedance, and improved control robustness. Existing hybrid actuators include haptic devices utilizing magnetorheological (MR) brakes in parallel with DC Motors [10]. Passive Eddy current dampers and back EMF properties of electric motors are also used to provide variable damping sources in parallel with active electric motors to provide increased control robustness and aid in rapid actuator movements [11][12]. Series damping actuators and series clutch actuators utilize clutches to isolate the high impedance gear head in a similar way to SEA's [13][14]. Parallel combinations of clutch's and SEA's have been shown to improve actuator energy efficiency [15][16]. Mckibbin muscles and mini brakes were shown to increase actuator performance under large impacts [17]. Performance gains from hybrid actuation are considerable, yet hybrid actuators often still suffer from nonlinearities associated with passive actuators, a low control bandwidth, and oftentimes an inherent imbalance between passive and active actuator torque capability [10].

II. A Balanced Hybrid Active-Passive Actuator

To address the limitations of existing actuation and enable human-robot applications that require high force and high power while also maintaining the physical characteristics important for safe and effective physical interaction we propose the use of a balanced hybrid actuation approach [18][19], conceptually shown in Fig. 1. In prior work we have shown that balanced hybrid actuation can increase the rendering range of kinesthetic haptic devices. In this paper, we extend the application of balanced hybrid actuation to general physical human-robot applications and investigate its potential benefits regarding performance and safety.

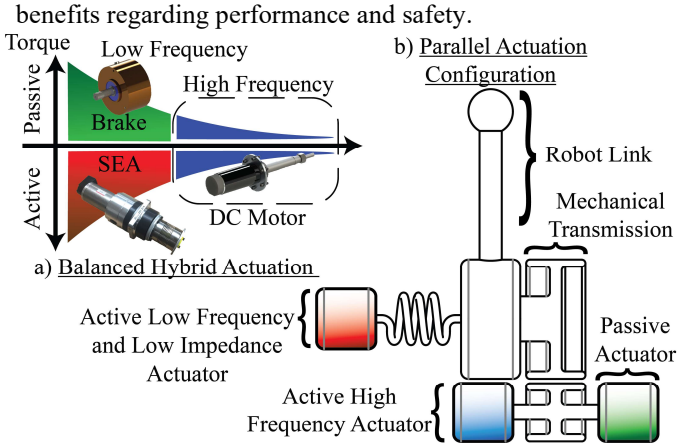

Fig. 1 a) The balanced hybrid actuation concept: active and passive torque partitioning as a function of frequency. b) Overview of the balanced hybrid active-passive actuation approach.

A. Actuation Concept

Balanced hybrid actuation combines energy-absorbing high-force low impedance passive actuation, high power low impedance active compliant actuation, and active high frequency actuation together. Balanced hybrid actuation, improves upon prior hybrid actuators by not only providing a large range of active and passive force magnitudes, but a large frequency range of active and passive torques.

In the context of human-robot interaction, including passive actuation helps to reduce power consumption, aid in servoing movements, and safely increase the dissipative power capability of the actuator. The inclusion of active compliant actuation and a high frequency active actuator provides large bandwidth active torque capabilities and may be used to compensate for slower response speeds and nonlinearities typical of passive actuators, while maintaining a low output impedance essential for safety. A key component to our balanced hybrid actuation concept is the constructive combination of all three actuators in parallel, made possible by the low output impedance characteristics of each element of the combined hybrid actuation. The combined actuation is balanced in regards to frequency, providing low-impedance actuation over a wide bandwidth, and in regards of torque production, providing high active and passive torque and power output. Finally, the low output impedance of the combined actuation approach greatly reduces impact loads during uncontrolled collisions, essential for safe human- robot interaction.

B. A One Degree of Freedom Testbed

A one degree of freedom actuation testbed, shown in Fig. 2, was constructed to evaluate the balanced hybrid actuation concept. The testbed incorporates a (1) series elastic actuator (SEA) as the high power, low impedance active compliant actuation, (2) a particle brake as the energy-absorbing, high-force, low impedance passive actuation, and (3) a low-inertia DC motor as the fast, low-power active actuation.

High-power active actuation: SEA's incorporate a compliant element at their output and use feedback to create a low-impedance torque source, effective below the SEA's closed-loop bandwidth, while the compliant element ensures low output impedance at high frequency (important for safety). In our testbed, the SEA torque is derived from a brushless DC motor in series with a high-ratio speed reducer. The speed reducer helps to increase the power density of DC motor by allowing the motor to operate at higher speeds while the SEA compliance and feedback control reduces the output impedance of the DC motor and speed reducer to safe levels.

High-power passive actuation: Including the particle brake at the output allows for a broad frequency range of passive torques of a similar magnitude to the SEA. However, a particle brake's response time is generally slower than DC motors especially as the torque capacity of the brake increases. Consequentially, the brake is primarily responsible for producing lower frequency passive torques. Particle brake rotors have low inertia and do not significantly impact the links inertia and safety of the actuator.

© 2021 IEEE. Personal use of this material is permitted. Permission from IEEE must be obtained for all other uses, in any current or future media, including reprinting/republishing this material for advertising or promotional purposes, creating new collective works, for resale or redistribution to servers or lists, or reuse of any copyrighted component of this work in other works

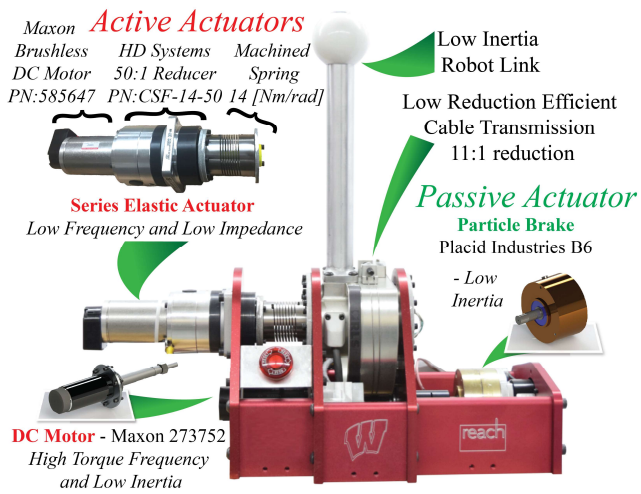

Fig. 2 A one degree of freedom balanced hybrid actuation test bed with a SEA, brushed DC motor, and particle brake arranged in parallel used to explore the actuation concept.

Fast, low-power active actuation: Series elastic actuators are most effective as low impedance torque sources below the flexible mode frequency introduced by the series elastic element while particle breaks are limited by their relatively slow response time. To combat this effect we include a small DC motor to recover high-frequency capability.

The DC motor is primarily responsible for high frequency content that the SEA and particle brake are unable to produce. The reflected inertia of the small DC motor has been shown to have little impact on robot safety in [5], if an efficient and low reduction speed reducer is used. We chose a stiff and efficient 11:1 cable reduction, Fig. 2, which connects each component in parallel. The direct connection to the output link allows the DC motor to produce torques above the SEA's flexible mode.

In the following sections we use the testbed described above to explore the potential benefits of the proposed actuation approach. We describe a candidate control approach in section III, explore performance benefits in section IV, and explore safety characteristics in section V.

III. HYBRID ACTUATOR CONTROL

Many tasks performed by cooperative robots today are at their core tracking and position control problems. Our hybrid actuator needs a control strategy that can address the redundant and nonlinear nature of our actuator and yield a high level of tracking performance while allowing us to explore its advantages. In trajectory tracking often the feed forward path contributes the majority of the control effort to actuators. Consequently, utilizing the passive actuator in feed forward control allows us to capture much of its tracking benefits while avoiding potential problems resulting from including a nonlinear actuator in our feedback control path. To this end we have implemented a control approach that incorporates feed forward control, leveraging the torque capabilities of all three component actuators, in combination with an active-only feedback controller. The active-only state feedback controller is tuned using a solution to the infinite-horizon Linear Quadratic Regulator (LQR). A high-level diagram showing the control structure is shown in Fig. 3.

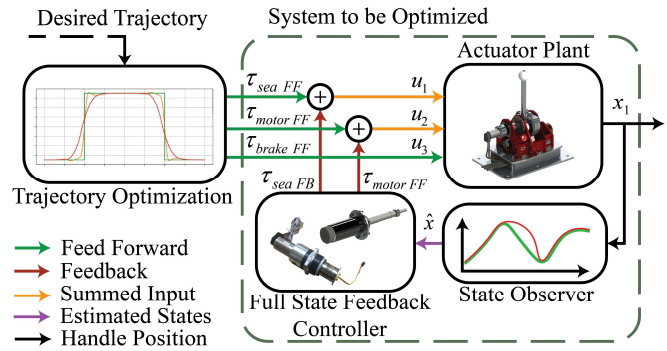

Fig. 3 High level overview of the balanced hybrid active passive actuation control structure.

A. Hybrid Feed Forward Control by Trajectory Optimization

To evaluate the proposed balanced active-passive actuation, it is instructive to examine specific tracking scenarios where its inherent characteristics suggest that it could provide significant benefits.

However, we cannot rely on classical control techniques to formulate the specific feedforward torque profiles for the component actuators due to the nonlinear nature of hybrid actuation. Instead, we turn to optimal control and, more specifically, an offline trajectory optimization method known as direct collocation, described in more detail in appendix A. Trajectories generated with direct collocation can be computationally costly, but not prohibitively so, making the approach suitable for fast, offline computation. For example, for the trajectories generated in this work (spanning motions of up to 4 seconds), did not exceed 30 seconds of the computation time when computed on a standard desktop computer. Using direct collocation, the actuation feed forward signals in this paper were pre-computed offline and applied online via interpolation and a lookup table. Online disturbance rejection is mainly left to the active actuators LQR controller.

IV. HYBRID ACTUATOR PERFORMANCE EVALUATION

To explore the potential benefits of the proposed hybrid actuation approach, we investigate three specific tracking scenarios including the following:

A. Time Optimal Control: Investigate improvements in time to target performance resulting from large high-power passive decelerations.

B. Minimum Energy Control: Investigate potential energy savings and/or control efficiency resulting from the low energy costs of the passive actuation.

C. *Tracking Error–Control Effort Tradeoff*: Explore hybrid actuation control with a more traditional LQR based cost function.

A. Time Optimal Control

Hybrid actuators could help to enable high power high force cooperative robotics because of their ability to create large dissipative forces. Enabling a robot to decelerate faster could increase the capability of a robotic manipulator in terms of its achievable trajectories and the maximum power flow that it can achieve.

© 2021 IEEE. Personal use of this material is permitted. Permission from IEEE must be obtained for all other uses, in any current or future media, including reprinting/republishing this material for advertising or promotional purposes, creating new collective works, for resale or redistribution to servers or lists, or reuse of any copyrighted component of this work in other works

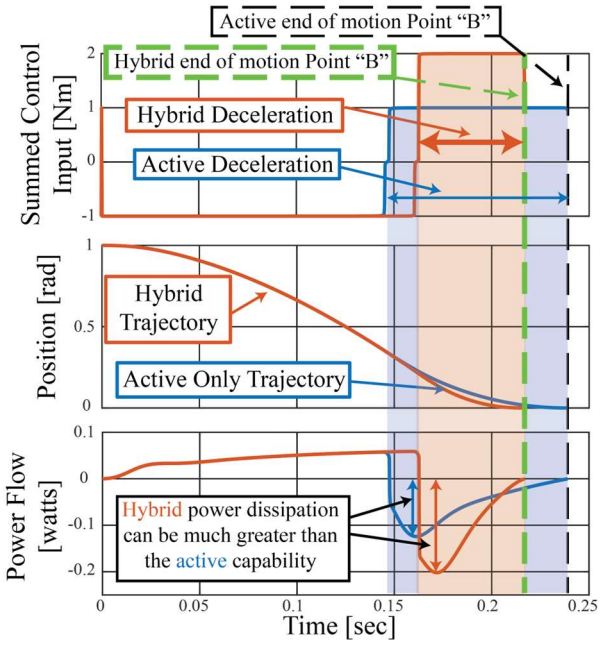

Fig. 4 Active only and hybrid time optimal control profiles generated via trajectory optimization. The hybrid actuator moves from point "A to point "B" faster than the active actuator and achieves a higher power movement while decelerating.

A convenient way to observe this impact of the hybrid actuator is through what is known as time optimal control. Time optimal control problem finds a trajectory that moves the systems initial states, point "A", to a final state, point "B", in the minimum amount of time. Actuation saturation limits must be included to make the problem well posed. In the spirit of our balanced hybrid actuator we assumed the combined active actuators and passive actuators have equal saturation points (i.e. 1 Nm for active and passive). Trajectories resulting from time optimal control of our hybrid actuator are compared to the active only portion of our actuator in Fig. 4.

Unsurprisingly, the hybrid actuator arrives at its destination point "B" faster than the active only actuator. The hybrid actuator does so by taking advantage of the dissipative torque capability of the passive actuator. Plotting mechanical power flow at the robot's link, shows the hybrid actuator's trajectory achieved a dissipative mechanical power flow nearly double the active actuators. This occurs during the deceleration phase of the hybrid actuators trajectory and is due to the slightly increased peak handle velocity and because of the greatly increased braking capability of the hybrid actuator. The time optimal control formulation shows that it is advantageous to use the passive component of hybrid actuators to safely achieve high power dissipative movements like decelerating a large mass; which could be essential to the performance of high power high force cooperative robots.

B. *Minimum Effort or Minimum Energy Control*

Another potential benefit of our balanced hybrid actuator are the energy savings that passive actuators can achieve. That is to say, when properly controlled, Fig.5, a hybrid actuator achieves a given trajectory more energy efficiently than a traditional active actuator. Minimum energy control or minimum effort control provides a framework to reduce the energy usage of the actuator as a whole while tracking a trajectory. The method minimizes the weighted sum of the actuators control effort squared [20] and is explained in greater detail in Appendix A. We chose a sine wave as a representative trajectory to show the energy saving benefits of our hybrid actuator. Comparing the summed squared actuation costs and the integral of each actuator's instantaneous power magnitude, Table 1, shows the hybrid actuator can achieve the desired trajectory more efficiently in terms of both the minimum control effort cost function and in terms of actual total mechanical energy transferred by the actuator. As shown in Fig. 5b and 5c, the passive actuator is contributing almost half the torque that the DC motor would otherwise be contributing. Again, we see it is advantageous to use the passive actuator, this time in terms of energy, to decelerate the robot's link.

TABLE I - COMPARISON BETWEEN ACTIVE ONLY AND HYBRID MINIMUM ENERGY CONTROL COSTS FOR THE SAME 5 HZ SINE TRAJECTORY.

Actuation Type	Min. Cost Function	Integral of absolute value of mechanical power
Active Only (SEA and Motor)	~10300	4.5623 [joules/per cycle]
Hybrid (SEA Motor and Brake)	~7000	3.2431 [joules/per cycle]

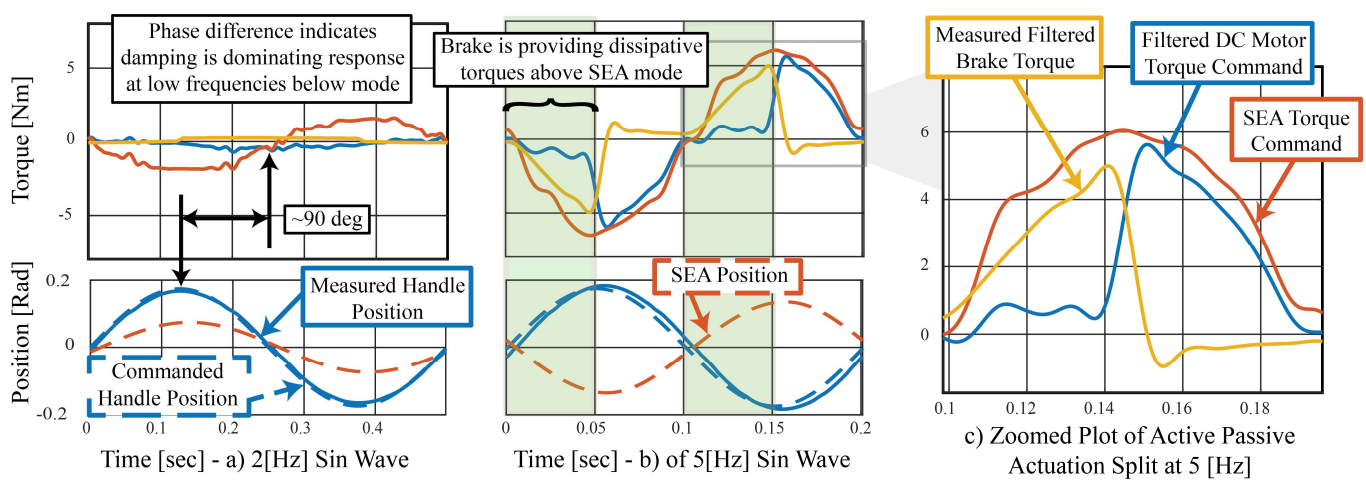

Fig. 5 Comparison of Experimental tracking of a sine wave using minimum energy control actuator outputs compared to the optimization output. a) The 2 Hz trajectory is below the flexible mode, or natural frequency, of the SEA. b) The 5 Hz trajectory is above the SEA flexible mode. c) The zoomed 5 Hz trajectory shows how the DC motor and brake begin to dominate the actuators torque response at higher frequencies. Results were obtained using active actuators in the feedback loop for disturbance rejection. A zero lag low pass filter is applied to the torque waveforms after data collection.

© 2021 IEEE. Personal use of this material is permitted. Permission from IEEE must be obtained for all other uses, in any current or future media, including reprinting/republishing this material for advertising or promotional purposes, creating new collective works, for resale or redistribution to servers or lists, or reuse of any copyrighted component of this work in other works

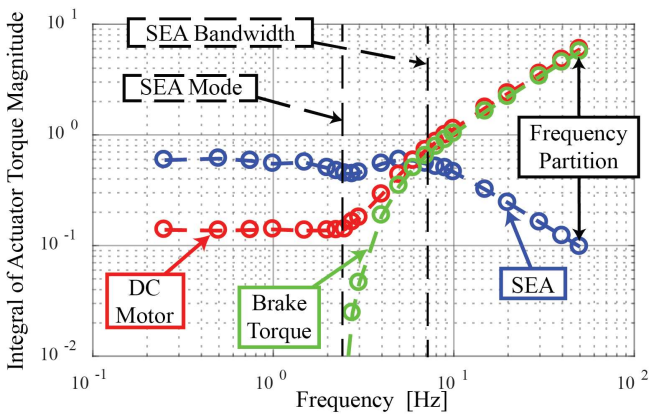

Fig. 6 Actuator frequency partitioning due to minimum effort/energy control (plotted integral of the absolute value of each actuators torque contribution from a single sine wave cycle). Note, the brake and DC motor nearly split the actuation costs equally above the SEA flexible mode.

Frequency partitioning between actuators, shown in Fig's 5 and 6, is an interesting consequence of minimizing actuation effort. Results show, it is most efficient to use the SEA as a low frequency torque source below its mode. The brake does not contribute significantly at low frequency either, for this specific trajectory, because the actuator is primarily overcoming internal damping. Consequently, the phase of the DC motor at 2 Hz is approximately 90 degrees out of phase with the handle position. In the case of sine wave trajectories, the brake and DC motor work together to generate higher frequency torques above the SEA's flexible mode. It is important to note, that the high frequency content of the brake is limited in reality as is indicated in Fig. 2. The results presented in Fig. 6 are obtained directly from the optimization output which does not account for high frequency limitations on both the DC motor and the brake. In summary, Fig. 6 shows a clear interplay between low and high frequency actuators and our control approach is effective at reducing actuation and energy costs while tracking a given trajectory.

C. *A Tradeoff Between Tracking and Control Effort*

Thus far, we have seen hybrid behavior take advantage of the dissipative attributes of the passive actuator to decelerate the robot link. However, it can be advantageous to use the passive actuator prior to the acceleration phases of trajectories. As we will show, the SEA and particle brake can work together to store potential energy in the SEA's compliant element which in turn can be used to increase resulting tracking acceleration. This synergistic behavior is of particular interest because it allows the system to track trajectories that required rapid accelerations, beyond the capabilities of each actuator individually.

To investigate this potential synergy, we can use a feed forward optimization approach inspired by LQR control where the optimization cost function trades off tracking error and control effort. By heavily weighting the handle position error in the cost function, the actuator will be forced to track a specified trajectory while creating a feasible trajectory in the process. This method is discussed in Appendix A.

Using this feed forward formulation, it is interesting to examine the behavior of the hybrid actuator when attempting to track a square wave, the experimental results of which are shown in Fig. 7. The brake is used during both the acceleration and deceleration phases of the approximate square wave and during low velocity portions of the trajectory. Interestingly, during the pre-acceleration phase energy is stored in the SEA spring by using the brake to hold the handle in place at the tracking reference while the SEA servos forward towards the new equilibrium position.

The brake then releases the stored spring energy. Following this, a high frequency free movement handle acceleration phase occurs where the DC motor supplies some high frequency torque. Finally, the brake is engaged, dissipating energy which decelerates the link. As the overall balanced hybrid actuation concept suggests, the brake and SEA are primarily working together to produce the desired motion while the DC motor fills in where the other actuator's dynamics prevent them from producing constructive torque or where it is not desirable to use the SEA or brake.

In addition to the benefits described, the synergistic behavior between the brake and SEA at low frequencies can be used to help to solve velocity saturation problems common to SEA [21]. In fact, we can accentuate the interplay between the SEA and brake by penalizing the SEA mass velocity in our cost function. The result is a slower SEA position response while maintaining the desired fast output position response. Avoiding SEA velocity saturation is achieved by storing more energy in the SEA spring and as a result higher brake activation levels prior to the output link movement.

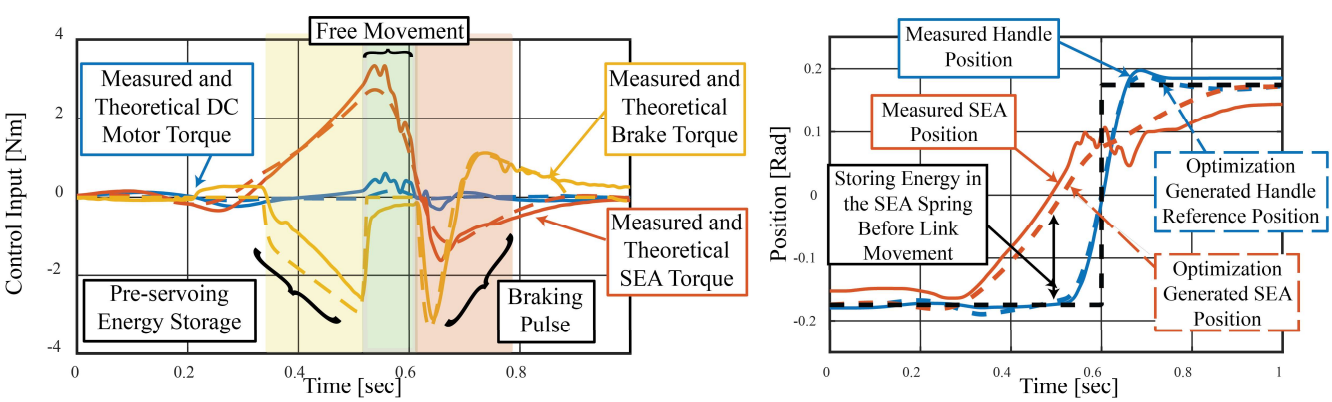

a) Theoretical and experimental torque response

b) Position response through half of a square wave

Fig.7 Experimental (solid lines) and optimization results (dashed lines) b) Each actuators torque contribution predicted by the optimization output (dashed lines) and measured experimentally data (solid lines) a) tracking a square wave using a LQR based cost function which trades off between tracking error and actuation effort with active only state feedback control. (Unmodeled gravity and friction disturbances cause the steady state error at the end position)

© 2021 IEEE. Personal use of this material is permitted. Permission from IEEE must be obtained for all other uses, in any current or future media, including reprinting/republishing this material for advertising or promotional purposes, creating new collective works, for resale or redistribution to servers or lists, or reuse of any copyrighted component of this work in other works

V. Hybrid Actuator Safety Evaluation

Clamping and blunt impacts are the predominate methods by which robots injure people [22]. Clamping injuries occur in robot joints or with robots against another object. Impact injuries arise from high inertia robots impacting people at high velocity and will be the focus of the safety study in this work. Research investigating these impacts has shown that the reflected inertia of an actuator contributes significantly to the safety of a robot overall and reducing the reflected inertia can help to make a robot safer especially at high velocities. The design of a SEA directly addresses this safety risk by introducing a series elastic element between the load (i.e. robot link) and the actuator, significantly reducing the effective inertia of the actuator (in regards to impact) and is widely considered a safe robotic actuator [23].

Our proposed combined active-passive hybrid actuator differs from a SEA actuator with the addition a small DC motor and passive actuator. Previously it has been shown [3] that adding a small DC motor in parallel with an SEA actuator can be accomplished without degrading the impact safety of a manipulator, assuming that the small motor and its associated reduction have low reflected inertia, as is the case with the actuation approach proposed here. The question remains whether adding a passive actuator might affect impact safety. To this end, we have conducted an experimental impact test which compares the active portion of the balanced hybrid actuation concept to the full hybrid actuator. The results of the experiment are used to validate an impact simulation. The active and hybrid actuator impact simulation is repeated on a full-size collaborative robot to study impact safety under more realistic conditions.

A. Hybrid Actuator Impact Experiment and Validation

The impact test set up, shown in Fig. 8, consists of a weighted pendulum instrumented with an encoder (US digital PN:E5-5000-375-IE-D-H-D-B) and an accelerometer (Analog devices PN:EVAL-ADXL325Z). The pendulum also includes a leaf spring to augment the interface stiffness between the robot link and the pendulum.

During the impact tests the robot was controlled using the approach described in section IVB, such that the impact velocity was constant over the set of tests performed. The testbed position trajectory was set to ensure that the passive actuator was engaged at the moment of impact. To evaluate the effect of the passive actuator (i.e. particle brake) on impact safety, we compared the impact results of the full hybrid actuator to that of the active portion alone. During the active-only experiment the particle brake was physically decoupled.

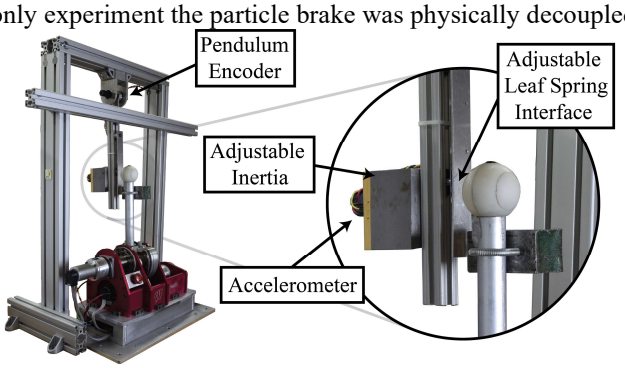

Fig 8. Experimental impact test setup with instrumented pendulum.

As seen in Fig 9, the acceleration of the pendulum following impact with the full hybrid actuator testbed as compared to the acceleration following impact with the active only testbed are approximately equal, demonstrating that the addition of the passive actuator has little effect on the peak measured acceleration.

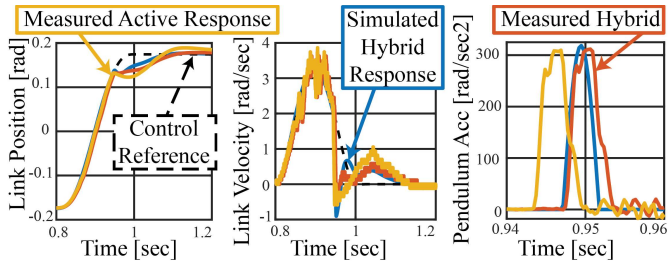

Fig. 9 Comparison of active only balanced hybrid and simulation impacts.

B. Balanced Hybrid Cobot Impact

While the test results are informative, the impact safety of a full size hybrid robot and human tissue is still in question. To address this, we developed a simulation, validated using the test results described above (see Fig 9), with parameters set to represent a head impact with a full-size collaborative robot, in this case a universal robots UR5 configured in its home position. A human head and skull stiffness are estimated at 6 kg and 37000 kg/m, respectively, and are used as the impacted mass and interface stiffness, respectively [24]. Finally, the SEA stiffness and inertia were calculated and set in accordance with the guidelines from [18]. The head acceleration profile, and peak acceleration are shown in Fig. 10. In addition, the Head Injury Criteria (HIC) [22], a common metric used to assess the likelihood of serious head injury, was evaluated to allow a direct comparison of the actuation impact characteristics.

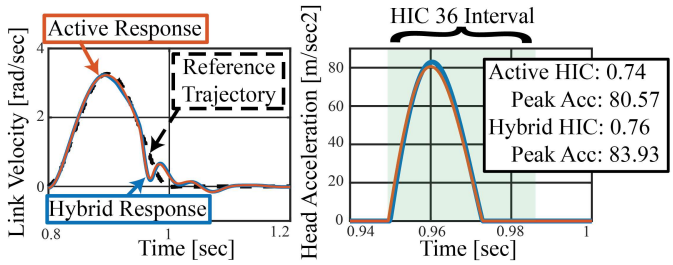

Fig. 10 Simulated head acceleration profile resulting from full size active and hybrid cobot collision.

As seen in Fig 10, the simulation demonstrates that for an average human head and skull stiffness the hybrid actuator performs nearly identically to the active only cobot in terms of the resulting peak acceleration and HIC.

VI. Conclusion and Future Work

Our balanced hybrid human friendly robotic actuator has many benefits. Designing the individual actuators in parallel allows us to size them to be of comparable torque capability which in turn grants the actuation method a high dynamic range while maintaining a low output inertia necessary for safety in cooperative robotics. Our experiments show, adding a passive actuator can increase the actuation and power absorption capability of the hybrid actuator, enable lower energy costs, and help to overcome other actuation limitations like SEA velocity saturation in a safe manor.

© 2021 IEEE. Personal use of this material is permitted. Permission from IEEE must be obtained for all other uses, in any current or future media, including reprinting/republishing this material for advertising or promotional purposes, creating new collective works, for resale or redistribution to servers or lists, or reuse of any copyrighted component of this work in other works

Despite the notable advantages, balanced hybrid actuation brings comes with some limitations. The first being the added complexity of combining three actuators in parallel. Another disadvantage is the added friction and weight of the DC motor and brake. With that said the presented design was not optimized for weight and additional research into passive actuation itself could help to reduce weight and latent friction in the current design.

Future work on our hybrid actuator includes an investigation of multi-phase optimization and model predictive control, to utilize the full brake model in our trajectory optimization program and to enable DC feedforward brake torques. Building a multi degree of freedom testbed to show how hybrid actuators can benefit higher degree of freedom systems would be an important contribution as well.

APPENDIX A – TRAJECTORY OPTIMIZATION METHODS

Direct collocation is a numerical method of trajectory optimization which transcribes the dynamics of our system, shown in Fig. 11, into constraints in an optimization problem. Time is discretized at knot points and the dynamics of our system constrains the states at each knot point. A full description of the direct collocation method is out of the scope of this paper. However, [1] provides an excellent introduction to the method. In this work we used Julia, JuMP, and IPOPT to transcribe and solve the nonlinear optimization problems.

As stated previously direct collocation relies on the transcription of the system dynamics into constraints. It is important to explore the necessary level of model complexity as a part of the transcription process. While the actual system is more complicated than the two-mass system shown in Fig. 11a calculating a lumped equivalent inertia and damping at the output of the SEA speed reducer and at the robot's link proved to be an effective model for feedforward control of the actuator.

Including the series elastic actuator controller in the optimization problem improved experimental results dramatically. The full dynamics of the particle brake can be represented by a modified dahl friction model as shown in [23]. Instead, we chose to represent the nonlinear brake dynamics with a smoothed version. A sigmoid function, shown in Fig. 9b, enforces a purely dissipative constraint on the torque contribution of the brake while allowing for the use of a gradient based nonlinear optimizer.

A. Time Optimal Control Formulation

The time optimal control problem can be solved using direct collocation, as shown in (1-8), where the time in-between collocation points is treated as a decision variable and is minimized. The time in-between collocation points is included in the Euler integration numerical approximation of the linear state equations shown in (2). Time optimal control must include actuation saturation limits to be well posed as shown in (4-6) and have a solution.

Minimize: $$J = T_S T \quad (1)$$

Subject to: $$For: k = 0,1,\ldots T-1$$

$$\frac{(x_{k+1} - x_k)}{T_s} = Ax_k + Bu_k \quad (2) \qquad u_{3_k} = \frac{-2u_{b_k}}{\left(1+e^{-\sigma\dot{x}_1}\right)} + u_{b_k} \quad (3)$$

$$-\tau_{A1_{sat}} \le u_{1_k} \le \tau_{A1_{sat}} \quad (4) \qquad -\tau_{A2_{sat}} \le u_{2_k} \le \tau_{A2_{sat}} \quad (5)$$

$$0 \le u_{b_k} \le \tau_{b_{sat}} \quad (6) \qquad x_0 = \begin{bmatrix}1 & 0 & 1 & 0 & 0\end{bmatrix} \quad (7)$$

Where: $$x_T = \begin{bmatrix}0 & 0 & 0 & 0 & 0\end{bmatrix} \quad (8)$$

T_S = Sample Time $\quad$ T = Number of knot points

k = Knot point index $\quad$ x_k = The state vector

A = State space matrix $\quad$ B = State space matrix

$u_k = \begin{bmatrix}u_{1_k} & u_{2_k} & u_{3_k}\end{bmatrix}^T$ = Control vector at knot point k

u_{1_k} = SEA torque $\quad$ u_{2_k} = DC motor torque

u_{3_k} = Brake Torque Output $\quad$ u_{b_k} = Brake Model Input

$\tau_{A1_{sat}}$ = SEA saturation limit $\quad$ $\tau_{A2_{sat}}$ = Motor saturation

$\tau_{b_{sat}}$ = The particle brakes torque saturation limit

x_0 = Initial state vector $\quad$ x_T = Final state vector

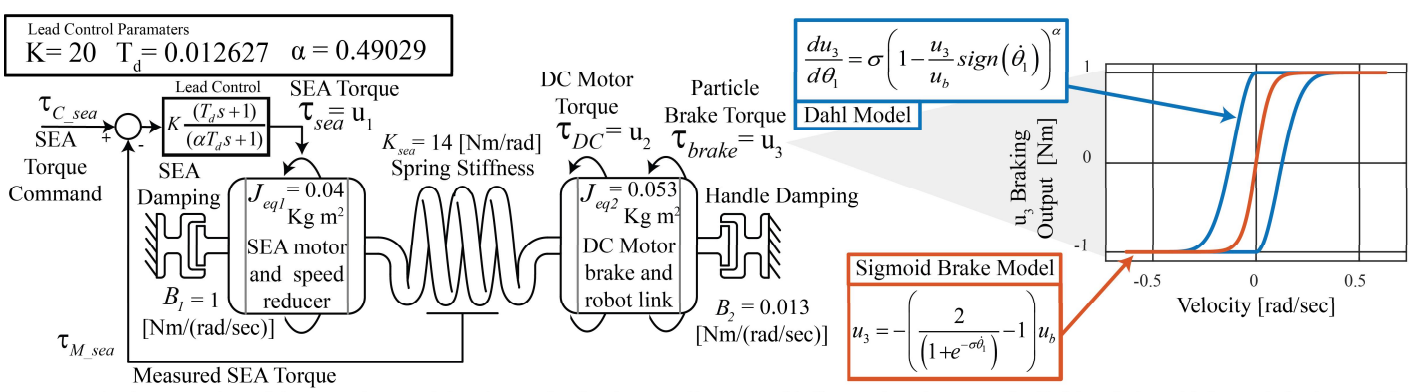

a) Linear portion of the actuation model and SEA feedback controller $\quad$ b) Comparison between the Dahl and sigmoid dynamic brake models

Fig. 11 a) Diagram of the equivalent two mass actuator system with equivalent SEA and robot link inertia. For optimization purposes the system includes the series elastic actuator controller (single lead) and the state feedback position controller. b) Comparison of the brake model friction force output showing the differences between the more accurate dahl model and the sigmoid brake model used in the optimization formulation. Dahl: σ= Model stiffness, α=hysteresis shape parameter. Sigmoid: σ= slope at origin, ub= steady state brake torque command

© 2021 IEEE. Personal use of this material is permitted. Permission from IEEE must be obtained for all other uses, in any current or future media, including reprinting/republishing this material for advertising or promotional purposes, creating new collective works, for resale or redistribution to servers or lists, or reuse of any copyrighted component of this work in other works

B. Minimum Energy Optimal Control Formulation

Minimum energy trajectory optimization minimizes the actuation costs to achieve a given trajectory. The cost function utilizes a matrix "R" shown in (9) which weights the relative costs of each actuator. In the trajectories shown we assign the relative weight of the SEA actuator and the DC motor as the ratio of the transmission ratios. That is to say that the ratio of R1 to R2 is set to be 4.7:1. Our justification comes from the effective gain of each actuator themselves. The brake is more efficient at producing torque than either the SEA or the DC motor within its limited dynamics and we penalize the brakes actuation much less than either actuator. The ratio of R2 to R3 is 10:1 for all the plots in this work.

Minimize: $$J = u^T diag\left(\begin{bmatrix} R_1 & R_2 & R_3 \end{bmatrix}\right) u = u^T R u \qquad (9)$$

Subject to: (2) and (3) $\qquad For: k = 0,1,...T-1$

$$x_{1_k} = x_{1ref_k} \qquad (10)$$

Where:

R_1 = SEA penalty $\qquad R_2$ = DC motor penalty

R_3 = Brake penalty $\qquad x_{1ref_k}$ = Joint Position Reference

C. Tracking and Control Effort Tradeoff

The LQR style cost function, shown in (11), allows us to investigate the tradeoff between tracking states and the control effort needed to do so. Heavily penalizing the first element in the error vector with the weight Q1, causes the actuators output position to track the desired position closely. Penalizing or increasing Q4, the weight associated with the SEA velocity state, helps to address SEA velocity saturation like described in previous sections.

Minimize:

$$\begin{aligned} J &= e^T diag\left(\begin{bmatrix} Q_1 & Q_2 & Q_3 & Q_4 & Q_5 \end{bmatrix}\right) e \\ &\quad + u^T diag\left(\begin{bmatrix} R_1 & R_2 & R_3 \end{bmatrix}\right) u \qquad (11) \\ &= e^T Q e + u^T R u \end{aligned}$$

Subject to: (2) and (3) $\qquad For: k = 0,1,...T-1$

Where:

$e^T = \begin{bmatrix} e_1 & e_2 & e_3 & e_4 & e_5 \end{bmatrix}$ = State error vector

Q_1 = Joint position weight $\qquad Q_2$ = Joint velocity weight

Q_3 = SEA position weight $\qquad Q_1$ = SEA velocity weight

Q_5 = SEA lead controller weight

References

[1] H. Vallery, J. Veneman, E. van Asseldonk, R. Ekkelenkamp, M. Buss, and H. van Der Kooij, "Compliant actuation of rehabilitation robots," *IEEE Robot. Automat. Mag.*, vol. 15, no. 3, pp. 60–69, Sep. 2008

[2] G. A. Pratt and M. M. Williamson, "Series elastic actuators," in Proceedings 1995 IEEE/RSJ International Conference on Intelligent Robots and Systems. Human Robot Interaction and Cooperative Robots, Pittsburgh, PA, USA, 1995, vol. 1, pp. 399–406

[3] M. Zinn, B. Roth, O. Khatib, and J. K. Salisbury, "A New Actuation Approach for Human Friendly Robot Design," *The International Journal of Robotics Research*, vol. 23, no. 4–5, pp. 379–398, Apr. 2004,

[4] J. M. Hollerbach, I. W. Hunter, and J. Ballantyne, "A Comparative Analysis of Actuator Technologies for Robotics," in *The Robotics Review 2*, Cambridge, MA, USA: MIT Press, 1992, pp. 299–342.

[5] N. Hogan, "Impedance Control: An Approach to Manipulation," in *1984 American Control Conference*, San Diego, CA, USA, Jul. 1984, pp. 304–313.

[6] R. Q. Van der Linde, P. Lammertse, E. Frederiksen, and B. Ruiter, "The HapticMaster, a new high performance haptic interface," in Proc. Eurohaptics, 2002, pp. 1–5.

[7] D. P. Losey, A. Erwin, C. G. McDonald, F. Sergi, and M. K. O'Malley, "A Time-Domain Approach to Control of Series Elastic Actuators: Adaptive Torque and Passivity-Based Impedance Control," *IEEE/ASME Trans. Mechatron.*, vol. 21, no. 4, pp. 2085–2096, Aug. 2016

[8] N. Paine, "Design and Control Considerations for High-Performance Series Elastic Actuators," vol. 19, no. 3, p. 12, 2014.

[9] A. Bicchi and G. Tonietti, "Fast and 'Soft-Arm' Tactics," *IEEE Robot. Automat. Mag.*, vol. 11, no. 2, pp. 22–33, Jun. 2004.

[10] C. Rossa, J. Lozada, and A. Micaelli, "Design and Control of a Dual Unidirectional Brake Hybrid Actuation System for Haptic Devices," *IEEE Trans. Haptics*, vol. 7, no. 4, pp. 442–453, Oct. 2014.

[11] A. H. C. Gosline and V. Hayward, "Eddy Current Brakes for Haptic Interfaces: Design, Identification, and Control," *IEEE/ASME Trans. Mechatron.*, vol. 13, no. 6, pp. 669–677, Dec. 2008.

[12] A. Radulescu, M. Howard, D. J. Braun, and S. Vijayakumar, "Exploiting variable physical damping in rapid movement tasks," in *2012 IEEE/ASME International Conference on Advanced Intelligent Mechatronics (AIM)*, Kaohsiung, Taiwan, Jul. 2012, pp. 141–148.

[13] Chee-Meng Chew, Geok-Soon Hong, and Wei Zhou, "Series damper actuator: a novel force/torque control actuator," in *4th IEEE/RAS International Conference on Humanoid Robots, 2004.*, Santa Monica, CA, USA, 2004, vol. 2, pp. 533–546,.

[14] L. Chen *et al.*, "Optimal Control for Maximizing Velocity of the CompAct™ Compliant Actuator," p. 7.

[15] E. J. Rouse, L. M. Mooney, E. C. Martinez-Villalpando, and H. M. Herr, "Clutchable series-elastic actuator: Design of a robotic knee prosthesis for minimum energy consumption," in *2013 IEEE 13th International Conference on Rehabilitation Robotics (ICORR)*, Seattle, WA, Jun. 2013, pp. 1–6.

[16] D. F. B. Haeufle, M. D. Taylor, S. Schmitt, and H. Geyer, "A clutched parallel elastic actuator concept: Towards energy efficient powered legs in prosthetics and robotics," in *2012 4th IEEE RAS & EMBS International Conference on Biomedical Robotics and Biomechatronics (BioRob)*, Rome, Italy, Jun. 2012, pp. 1614–1619.

[17] D. Shin, X. Yeh, and O. Khatib, "A new hybrid actuation scheme with artificial pneumatic muscles and a magnetic particle brake for safe human–robot collaboration," *The International Journal of Robotics Research*, vol. 33, no. 4, pp. 507–518, Apr. 2014.

[18] P. Dills, C. Parthiban, I. Fufuengsin, and M. Zinn, "Design and Analysis of a High Performance Impedance Based Hybrid Haptic Interface," p. 3, 2018.

[19] C. Parthiban, P. Dills, I. Fufuengsin, N. Colonnese, P. Agarwal, and M. Zinn, "A Balanced Hybrid Active-Passive Actuation Approach for High-Performance Haptics," in *2019 IEEE World Haptics Conference (WHC)*, Tokyo, Japan, Jul. 2019, pp. 283–288.

[20] J. Klamka, Controllability and Minimum Energy Control, vol. 162. Cham: Springer International Publishing, 2019.

[21] D. W. Robinson, "Design and analysis of series elasticity in closed-loop actuator force control" PhD Thesis, Massachusetts Institute of Technology, Cambridge, MA, USA, 2000.

[22] S. Haddadin, A. Albu-Schaffer, and G. Hirzinger, "The role of the robot mass and velocity in physical human-robot interaction - Part I: Non-constrained blunt impacts," in *2008 IEEE International Conference on Robotics and Automation*, Pasadena, CA, USA, May 2008, pp. 1331–1338

[23] S. Robla-Gomez, V. M. Becerra, J. R. Llata, E. Gonzalez-Sarabia, C. Torre-Ferrero, and J. Perez-Oria, "Working Together: A Review on Safe Human-Robot Collaboration in Industrial Environments," *IEEE Access*, vol. 5, pp. 26754–26773, 2017.

[24] D. Shin, "A New Actuation Approach For Bio-Inspired Human-Freindly Robots" PhD Thesis, Stanford University, Stanford, CA, USA, 2000.

[25] M. Kelly, "An Introduction to Trajectory Optimization: How to Do Your Own Direct Collocation," *SIAM Rev.*, vol. 59, no. 4, pp. 849–904, Jan. 2017

[26] P. Dills, N. Colonnese, P. Agarwal, and M. Zinn, "A Hybrid Active-Passive Actuation and Control Approach for Kinesthetic Handheld Haptics," in *2020 IEEE Haptics Symposium (HAPTICS)*, Crystal City, VA, USA, Mar. 2020, pp. 690–697.

© 2021 IEEE. Personal use of this material is permitted. Permission from IEEE must be obtained for all other uses, in any current or future media, including reprinting/republishing this material for advertising or promotional purposes, creating new collective works, for resale or redistribution to servers or lists, or reuse of any copyrighted component of this work in other works